Magnetic Resonance Imaging (MRI)

Editors:

Kyle D. Wood, MD

Authors:

Michael Ahdoot, MD; Timothy Daskivich, MD, MSHPM

Last Updated:

Friday, March 3, 2023

Keywords

Tesla, prostate cancer, gadolinium, nephrogenic systemic fibrosis

1. Technical Considerations

1.1 Components of MRI Scanner

1.1.1 Magnet

The most important component of the MRI system is the magnet. **The strength of a magnet in an MRI system is rated using a unit of measure known as a Tesla** . The magnets in use today in most clinical MRI systems are superconducting magnets that create a magnetic field of 0.5-tesla to 3.0-tesla. For comparison, the Earth's magnetic field (25 to 65 microteslas) is exponentially less. There are also **three gradient magnets** inside an MRI machine. These magnets are much lower strength compared to the main magnetic field. While the main magnet creates an intense, stable magnetic field around the patient, the gradient magnets create a variable field, which allows different parts of the body to be scanned in different planes.[1]

1.2 Image Generation

Hydrogen atoms randomly spin on their axis around their individual magnetic field. When placed in the magnetic field of an MRI, the atoms line up in the direction of the field. When a radio frequency pulse is applied, the unmatched atoms spin the other way. The radio frequency pulse is turned off and the unmatched atoms return to their normal position, emitting the energy absorbed from the RF pulse. This energy sends a signal to a computer that uses mathematical formulas to transform the signal into images. [1]

1.3 MRI Sequences

1.3.1 T1-weighted MRI

T1-weighted scans refer to scans that depict differences in the spin-lattice (or T1) relaxation time of various tissues within the body**. Lattice refers to the environment that surrounds the spins.** T1 weighted scans work well for differentiating fat from water with **water appearing darker and fat brighter**. T1-weighted images are required to assess tissue enhancement with gadolinium based contrast agents. Macroscopic fat and hemorrhage (methemoglobin) are bright on T1-weighted images, and an additional frequency selective fat suppression pulse is required to differentiate between the two.[1]

1.3.2 T2-weighted MRI

T2-weighted scans refer to scans that depict differences in the spin-spin (or T2) relaxation time of various tissues within the body. **Fluid in the collecting system and urinary bladder is bright on T2-weighted images.**

1.3.3 Chemical Shift Dual In-phase and Out-of-phase Gradient Echo MRI

Chemical shift refers to the difference in precessional frequency between water and fat. Water and fat can rotate in-phase

or out-of-phase with one another. If water and fat are spinning in phase, the voxel (unit of graphic information defining a point on 3D MRI) maintains signal. If water and fat are spinning out of phase, the voxel loses signal. At 1.5 Tesla, the in-phase TE (echo time) is double the out-of-phase TE. Clinical applications of the chemical shift artifact include diagnosis of adrenal adenoma and other lesions that contain intravoxel/microscopic fat such as minimal fat angiomyolipoma or clear cell renal cell carcinoma.

2. Role of MRI

2.1 Advantages of MRI

The most important advantages of MRI include:

i. no need for nephrotoxic contrast material
ii. no radiation exposure to the patient
iii. high inherent soft tissue signal contrast
iv. imaging from any of the three orthogonal anatomical planes. **After ultrasound, MRI is the imaging modality of choice for patients with iodinated contrast allergy, mild renal insufficiency, and pregnancy.**

2.2 Limitations of MRI

Despite newer techniques:

i. examination times are still longer than computed tomographic (CT) imaging
ii. less spatial resolution
iii. associated with higher cost
iv. is **poor at detecting renal calculi** and calcifications
v. concentrated gadolinium results in magnetic susceptibility artifacts

3. Adverse Effects of MRI

3.1 Dangers of Magnetic Field

3.1.1 Biological Effects

Undergoing an MRI does not involve exposure to ionizing radiation, and **no clear long-term biological effects have been reported.** MRI is considered a safe technology since it changes the position of atoms, but does not alter their structure, composition, and/or properties.

3.1.2 Metallic Objects

Ferromagnetic foreign bodies, such as **shell fragments** or **metallic implants, such as surgical prostheses, ferromagnetic aneurysm clips, and cochlear implants** represent potential risks. Interaction of the magnetic and radio frequency fields with such objects can lead to trauma due to movement of the object in the magnetic field or thermal injury from radio-frequency induction heating of the object. **Pacemakers and defibrillators** have been a **contraindication to perform MRI.** However, starting in 2011, the Food and Drug Administration approved the first **MRI conditional device** that can be used safely under pre-specified conditions.[2] Coronary stents are considered MRI safe. A good resource for further information is **http://www.mrisafety.com/**

3.1.3 Noise

Acoustic noise generated due to the fast switching of currents within the gradient coils may be considerable**. Protective ear plugs/headphones** should be worn by patients (and accompanying personnel), particularly in systems operating at 1.5 Tesla and above.

3.1.4 Pregnancy

MR is not advised during the **first trimester of pregnancy or on MRI scanners higher than 1.5 Tesla**. This is

precautionary as no deleterious effects to mother or child are known. Gadolinium based contrast agents are generally avoided during pregnancy and lactation (FDA pregnancy category C).[3]

3.1.5 Claustrophobia

This may be encountered by patients with a prior history due to the tight confines of a MRI scanner. This can sometimes be ameliorated with oral sedatives. Alternatively, an open MRI is an option, but image quality may suffer.

3.2 Risks Associated with Contrast Material

3.2.1 Nephrotoxicity

Gadolinium-based contrast (GBC) agents greatly enhance MR images. Since iodinated contrast agents used with CT imaging are nephrotoxic, GBC agents have been preferentially used in patients with mild renal insufficiency. Patients are screened for renal disease prior to receiving intravenous GBC and an estimated glomerular filtration rate (eGFR) is calculated. The risk of nephrogenic systemic fibrosis is extremely low. Thus in most clinical situations the potential harms of delaying or withholding GBC is likely to outweight the potential harm. Numerous studies demonstrate that GBC agents, while **less nephrotoxic** compared to iodinated contrast, **may cause acute kidney injury (AKI)** in high-risk patients with CKD stages IV and/or V.[4]

3.2.2 Nephrogenic Systemic Fibrosis (NSF)

This disorder presents as a fibrosing disease of the skin and systemic organs **in patients with CKD stages IV and/or V**. Nearly 80% of patients have ESRD and are on dialysis, whereas the rest have primarily stage V CKD and AKI. Risk is associated with exposure to GBC and is increased with higher doses, cumulative exposure and type of GBC. If GBC agent exposure is required, **risks of NSF can be decreased by using the smallest dosage of a macrocyclic chelating agent (gadoteridol [ProHance®], gadobenate dimeglumine [MultiHance®], gadoterate meglumine [Dotarem®]), avoiding repeated exposure, and performing hemodialysis immediately following their MRI.**[4]

3.2.3 Gadolinium Deposition

In addition to risk of NSF, repeated exposures and higher cumulative doses of GBC have been recognized to show tissue deposition, particularly in the brain, with unknown long-term clinical implications. The United States Food and Drug Administration (FDA) issued a warning in 2017 for all GBC agents about the retention of gadolinium for months or years following intravenous administration. As part of this warning, the FDA has guided that patients should receive a medication guide prior to being given GBC agents.[5] A subset of GBC which are macrocyclic agents have been shown to result in lower levels of central nervous system deposition compared to linear based GBC agents.[6] The macrocyclic GBC agents are the ones typically used in prostate imaging.

4. Clinical Applications

4.1 Adrenal Gland

4.1.1 Anatomy

Typically the adrenal gland has a linear, inverted V or Y configuration. Normal adrenal glands range from 2-6 mm in thickness and from 2-4 cm in length.

4.1.2 Incidentalomas

An adrenal incidentaloma (unsuspected and asymptomatic mass) is commonly detected on a CT scan that was obtained for a different reason. A history of malignancy and the size of the mass are important factors to consider when evaluating the mass. A patient with a history of lung or renal cancer is at higher risk for an adrenal metastasis. Additionally, a size greater than 4 cm is more suspicious for malignancy than a smaller mass. The first step in evaluating the patient with the incidental adrenal mass is to determine if there are prior studies, and in a low risk patient, if the mass was present on an older study and has not changed in 1 year's time, it can be presumed to be benign. The majority of adrenal

incidentalomas are benign, and the majority represent lipid containing adrenal adenomas (**Figure 1**). Other adrenal lesions include cysts, myelolipomas, cortical carcinoma, pheochromocytoma, and metastases (**Figure 2**). Up to 70% of adrenal adenomas can be reliably diagnosed at unenhanced CT when they measure 10 Hounsfield Unit (HU) or less. When the adrenal mass measures greater than 10 HU on unenhanced CT or if the mass was detected on a routine contrast enhanced CT, the mass is indeterminant. Definitive characterization with CT washout study or chemical shift MRI may be considered. Chemical shift MRI uses dual echo in-phase and out-of-phase MRI images to detect intracellular lipid.[7] Signal intensity loss on out-of-phase sequences, when compared to in-phase imaging, signifies the presence of intracellular lipid and definitively identifies the lesions in question as an adenoma. Importantly, **CT washout studies are considered the gold standard** and demonstrate higher sensitivity and specificity than chemical-shift MR imaging in identifying adenomas.[7]

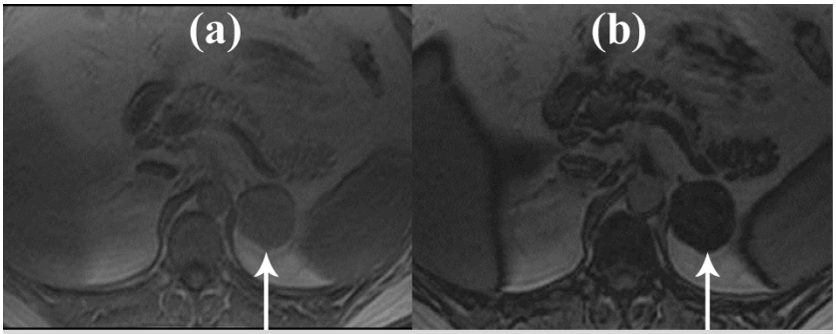

Figure 1: Axial T1 in-phase (a) and out-of-phase (b) images demonstrate a left adrenal mass (arrow) that homogeneously drops in signal on out-of-phase images in keeping with a left adrenal adenoma.

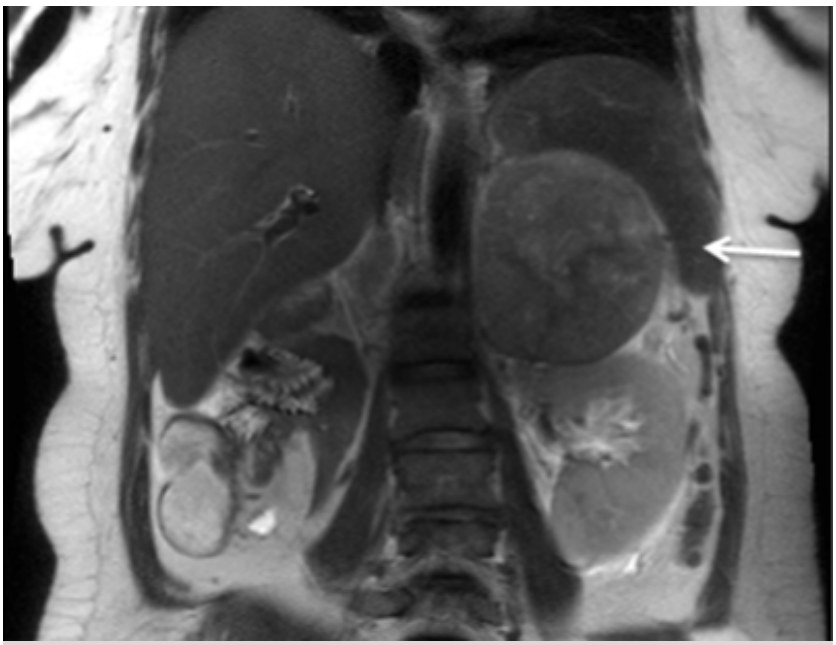

Figure 2: Coronal T2-weighted image of left adrenal metastasis (arrow) from renal cell carcinoma primary following prior right radical nephrectomy

4.1.3 Adrenal Cortical Carcinoma (ACC)

This tumor is usually large at presentation often measuring greater than 4 cm and demonstrating irregular margins often with internal hemorrhage and/or necrosis. It may be associated with tumor thrombus extending to the IVC (right side tumors greater than left), and para-aortic lymphadenopathy. The mass is typically iso- to hypointense to liver on

T1-weighted images, though can be T1 hyperintense due to hemorrhage. The mass is heterogeneously hyperintense on T2-weighted images due to necrosis and hemorrhage, and contains cystic areas. On gadolinium-enhanced images, adrenal carcinomas enhance heterogeneously. [8]

4.1.4 Pheochromocytoma

See **(Figure 3)**

Given their rich vascularity and low lipid content, pheochromocytomas do not exhibit signal dropout on out-of-phase sequences. Classically, pheochromocytomas **demonstrate bright signal intensity on T2-weighted imaging, termed the "light bulb" sign**.[9]

> **TAKE HOME POINT: When should an MRI be performed for an adrenal lesion? If the lesion is small and demonstrates benign imaging features, and there is no history of malignancy, the adrenal lesion should be presumed benign with no further imaging required. If the initial study is nondiagnostic for characterization of an adrenal adenoma, the next test can be either unenhanced CT or chemical shift MRI. MRI is preferred in pregnant patients and others in whom radiation exposure is a concern. If these tests are nondiagnostic, adrenal CT protocol with washout calculations can be performed.**

4.2 Kidneys

4.2.1 Anatomy

Magnetic resonance urography (MRU) allows all the anatomic components of the urinary tract to be thoroughly imaged in a single test. The main disadvantage of MRU compared to CT urography is decreased spatial resolution and its **poor ability to detect urinary calculi.** On **T1-weighted images** the kidney cortex appears bright and the medulla is dark. On **T2-weighted images,** urine appears bright.[10]

4.2.2 Renal Mass

See **(Table 1)**

Cortical renal tumors can be evaluated with MR imaging.[11] Dynamic contrast enhanced MRI can readily differentiate between solid and cystic renal masses. Additionally, different appearances on T1-weighted, T2-weighted, and chemical shift sequences and the different patterns of enhancement may allow for differentiation of the three most common renal cell carcinoma (RCC) subtypes (clear cell, papillary and chromophobe) with high accuracy.[12] (**Figure 3**). MRI is still **considered the gold standard for the evaluation of tumor thrombus** into the renal vein/inferior vena cava with accuracies ranging from 65-100%. On MR imaging, tumor thrombus will enhance. For the evaluation of **metastatic disease** MRI is highly sensitive and specific for bone metastasis (better than bone scintigraphy).[13]

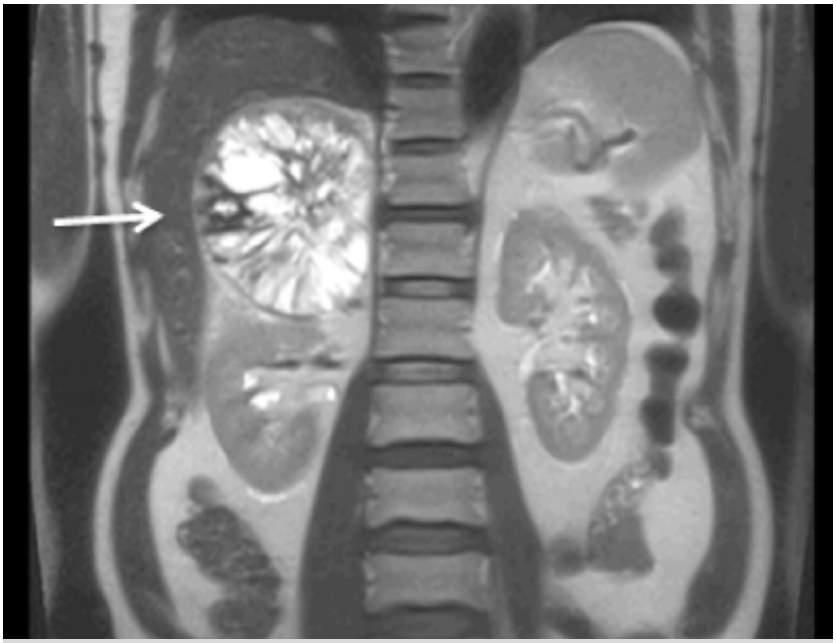

Figure 3: Coronal T2-weighted image of pheochromocytoma shows a large heterogeneously hyperintense right suprarenal mass (arrow).

Minimal fat angiomyolipoma (AML) versus clear cell renal cell carcinoma

While most AMLs can be reliably diagnosed when macroscopic/bulk fat is identified, accurate diagnosis of minimal fat AML is challenging.[14] Chemical shift MRI can show intravoxel fat (drop in signal on out-of-phase compared to in-phase imaging at 1.5 Tesla) in minimal fat AML, but this finding can also be present in clear cell carcinoma. Thus MRI cannot reliably differentiate minimal fat AML from a clear cell renal cell carcinoma. Certain MR imaging features favor minimal fat AML over clear cell renal cell carcinoma such as small size and homogeneous low signal intensity on T2-weighted images relative to renal cortex. Clear cell renal cell carcinomas typically appear increased in signal intensity on T2-weighted images and demonstrate areas of necrosis.

Table 1. Classic MRI Features of Renal Masses

T1	T2	CE	Diagnosis
Dark	Bright	Yes	RCC (Clear Cell)
Dark	Dark	Yes	RCC (Papillary)
Dark	Dark	Yes	AML Minimal Fat
Dark	Heterogeneous	Yes	RCC (Chromophobe)
Dark	Heterogeneous	Yes	Oncocytoma
Dark	Dark	Yes	Leiomyoma of Capsule
Bright	Variable	Yes	AML
Bright	Dark	No	Hemorrhagic Cyst

4.2.3 Urothelial Tumors

Urothelial carcinomas (UC) are typically isointense relative to the renal medulla on T1-weighted images, making the detection of small tumors in the collecting system difficult. **Bright signal intensity due to urine in the collecting system on T2-weighted images provides excellent soft-tissue contrast for the detection of these tumors, which are characteristically seen as hypointense filling defects** . Infiltrative UC can be seen on T2-weighted images as a hypointense soft-tissue mass infiltrating the renal parenchyma.[10] Additionally, diffusion weighted MRI and calculated ADC values may further assist in differentiating centrally located solid renal masses as renal cell carcinoma versus upper tract urothelial carcinomas; with lower ADC values tending to be associated with urothelial tumors of the renal collecting system over centrally located renal cell carcinomas.[15] This may help further direct potential role of endoscopic evaluation, percutaneous biopsy, or definitive surgical management.

4.2.4 Renal Function Assessment

See **(Table 2)**

Multiple techniques are in development to use the unique properties of MRI for the calculation of GFR and differential renal function.[16]

> **TAKE HOME POINT: When should an MRI be performed for renal pathology? MRI of the abdomen without and with IV contrast is indicated for imaging work up of an indeterminate renal mass and for assessment of tumor thrombus in the renal vein and IVC. Moreover, MRI depicts additional findings such as increased septa and wall thickness in complex renal cystic lesions compared to CT.**

Table 2: Renal Function Assessments Techniques using MRI

Technique	Summary
Dynamic contrast-enhanced (DCE) MRI	Capable of determining renal blood flow, GFR, and cortical and medullary blood volumes by measuring the transit of gadolinium contrast through the renal cortex, medulla, and collecting system.
Diffusion weighted MRI (DWI)	A non-invasive modality to characterize tissues based on Brownian motion of water molecules within them. Apparent diffusion coefficient (ADC) is a quantitative parameter calculated from DWI that combines the effects of capillary perfusion and water diffusion.
Blood oxygen level-dependent (BOLD) MRI	Exploits the paramagnetic effect of deoxyhemoglobin to indirectly measure renal oxygenation

4.3 Bladder

4.3 1 Anatomy

The urinary bladder wall is composed of four layers: urothelium, submucosa, muscularis propria (detrusor muscle) and the serosa.

4.3.2 Bladder Cancer

As with all patients, the use of MR imaging modalities for the bladder, especially for staging bladder cancer, is most helpful for patients with chronic kidney disease for whom IV contrast is not recommended or contraindicated. To achieve optimal bladder distension during MR imaging, it is ideal to have the patient void two hours prior to imaging. There have been some reports demonstrating that MR imaging may be more accurate in staging carcinomas of the bladder when compared to CT scanning due to its high soft-tissue contrast resolution, which allows for better differentiation between blad-der wall layers (see **Figure 6**).[17,18] Thus, theoretically, MRI may depict more clearly intramural tumor invasion as well as extravesical extension, allowing for differ-entiation between muscle-invasive and non-mus-cle-invasive bladder cancer—a key clinical distinction in the staging and treatment of patients diagnosed with bladder cancer (see **Figure 7**).

The urine on T1-weighted images demonstrates low signal intensity and the bladder wall demonstrates intermediate signal intensity (see **Figure 6**). Contrast enhanced imaging is performed dynamically (arterial phase followed by multiple venous phases). On the arterial phase, the tumor will enhance earlier than the bladder wall.

> **TAKE HOME POINT: When should an MRI be done for bladder pathology? The job of imaging is to identify muscle invasion, extravesical extension of tumor, and nodal metastases. MRI is superior to CT in delineating the lower pelvic anatomy and in detecting adjacent organ involvement by tumor. MRI can differentiate superficial from muscle invasive tumors. CT and MRI can identify abnormal lymph nodes, which appear enlarged or rounded. CT urography is superior to MR urography in detecting small urothelial tumors though recent advances in MR imaging have suggested equal detection for larger urothelial carcinomas.**[19,20]

Table 3. PI-RADS v2.1 Scoring of T2 Weighted images

PIRADS v2.1 – T2 (Suspicion for clinically significant cancer)	Transition Zone	Peripheral Zone
1 very low	Normal appearing TZ (rare) or a round, completely encapsulated nodule. (“typical nodule”)	Uniformly hyperintense signal intensity (normal)
2 low	A mostly encapsulated nodule OR a homogeneous circumscribed nodule without encapsulation. (“atypical nodule”) OR a homogeneous mildly hypointense area between nodules	Linear or wedge-shaped, hypointensity or diffuse mild hypointensity, usually indistinct margin
3 intermediate	Heterogeneous signal intensity with obscured margins Includes others that do not qualify as 2, 4, or 5.	Heterogeneous signal intensity or non-circumscribed, rounded, moderate hypointensity Includes others that do not qualify as 2, 4, or 5.
4 high	Lenticular or non-circumscribed, homogeneous, moderately hypointense, and <1.5 cm in greatest dimension	Circumscribed, homogeneous moderate hypointense focus/mass confined to prostate and < 1.5 cm in greatest dimension
5 very high	Same as 4, but ≥ 1.5 cm in greatest dimension or definite extraprostatic extension/invasive behavior	Same as 4 but ≥ 1.5 cm in greatest dimension or definite extraprostatic extension/invasive behavior

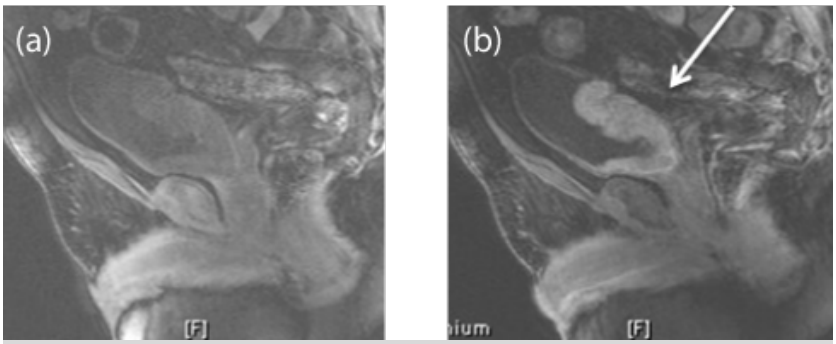

Figure 6: T1 and T2 Signal Intensity of Important Bladder Anatomy on MRI. Sagittal T1 fat suppressed imaging of the bladder prior to (a) and following intravenous contrast administration in the arterial phase (b) demonstrates rind-like thickening of the posterior bladder wall, that avidly enhances in keeping with a urothelial tumor.

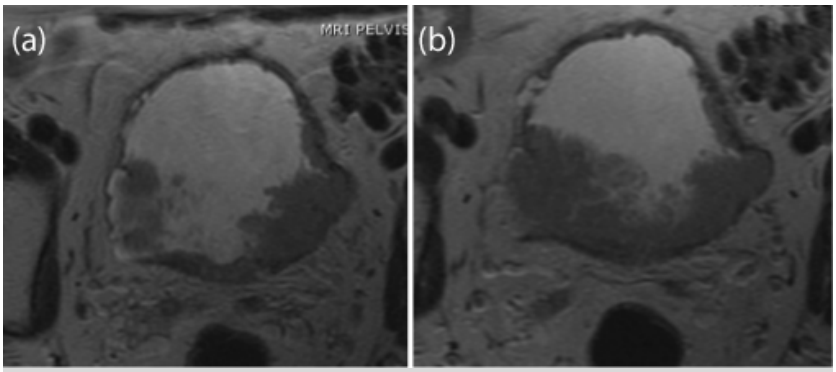

Figure 7: Axial T2-weighted imaging (a and b) of the bladder demonstrates high signal intensity urine and low signal intensity urinary bladder wall. The posterior circumferential polypoid bladder tumor is intermediate in signal intensity (b) and interrupts the low signal intensity bladder wall on the right and invades the perivesical fat, suggesting cT3 disease (a).

4.4 MRI of the Prostate

4.4.1 Anatomy

The application of MRI technology to image the prostate as part of the diagnostic, surveillance, and therapeutic workup for men with prostate cancer has increased dramatically over the past several years.[21] Indications for MRI of the prostate include cancer detection in the setting of an elevated PSA and negative prior biopsy, local and distant staging of intermediate/high risk patients, local recurrence post prostatectomy in patients with a rising PSA, active surveillance of patients with prostate cancer, and surgical planning (extraprostatic extension, impingement of the rectal wall, etc.).[22,23] Newer data has prompted the AUA to support[23] its use in the biopsy naïve setting for men with clinical suspicion for prostate cancer based upon PSA or other biomarker testing.[24,25,26,27]

In the diagnostic setting, using MRI to target lesions of interest on biopsy minimizes over detection of low-risk prostate cancers and increases yield of clinically significant prostate cancers compared with systematic biopsy alone,[28] though a combined systematic and targeted biopsy approach optimizes diagnostic accuracy.[29,30]

Factors that improve image quality include: allowing post-biopsy hemorrhage to subside by waiting 6-8 weeks after biopsy before performing MRI, evacuating the rectum of gas/stool to minimize artifact on DWI, and refraining from ejaculation 3 days prior to MRI to allow for adequate seminal vesicle distension.

For a basic understanding of prostatic MRI, it is important to review the zonal anatomy of the prostate. In young men, the peripheral zone (PZ) of the prostate comprises 75% of the prostate volume, and the central gland (CZ) - central and transition zones - makes up the remaining 25% of the prostate volume. T2-weighted imaging of the prostate displays these different zones, and its understanding is useful to help interpret prostate MRI.[31]

T1-weighted MR images are most useful in detecting post-biopsy hemorrhage. On T1-weighted fat suppressed images, hemorrhage will appear as increased signal intensity. Large field of view T1-weighed images that include the aortic bifurcation are also helpful in detecting lymphadenopathy and bone metastasis. T2-weighted images of the prostate play an important role in prostate cancer evaluation/detection since T2-weighted images can sharply delineate the PZ and CZ. Prostate cancer will typically appear hypointense on T1 and T2-weighted images.

Multiparametric prostate MRI is the addition of one or more functional MR imaging techniques to standard T1 and T2-weighted imaging. **These techniques include diffusion weighted imaging (DWI), MR spectroscopy, and/or dynamic contrast enhanced imaging (DCE)**.[31] Multiparametric MRI increases sensitivity and improves specificity for detection of prostate cancer. Patients are increasingly scanned with a phase array coil rather than an endorectal coil as imaging at 3T with phase array coil have shown comparable image results.

The American College of Radiology (ACR), European Society of Urogenital Radiology (ESUR), and AdMeTech Foundation developed the Prostate Imaging Reporting and Data System (PI-RADS) version 2 in 2015.[32] A newer iteration, or version 2.1, was released in 2019 as the most current guide to systematic scoring and reporting for suspicious lesion on prostate MRI.[33] The purpose of PI-RADS is to standardize acquisition, interpretation and reporting of prostate mpMRI studies. The categories range from PI-RADS 1 (clinically significant cancer is highly unlikely to be present) to PI-RADS 5 (clinically significant cancer is highly likely to be present). (**Table 3** and **Table 4**).

Table 4. PI-RADS v2.1 Scoring of Diffusion Weighted Images	
PIRADS – DWI (Suspicion for clinically significant cancer)	**Peripheral Zone or Transition Zone**
1 very low	No abnormality (i.e. normal) on ADC and high b-value DWI
2 low	Linear/wedge shaped hypointense on ADC and/or linear/wedge shaped hyperintense on high b-value DWI
3 intermediate	Focal (discrete and different from the background) hypointense on ADC and/or focal hyperintense on high b-value DWI; may be markedly hypointense on ADC or markedly hyperintense on high b-value DWI, but not both.
4 high	Focal markedly hypointense on ADC and markedly hyperintense on high b-value DWI; < 1.5 cm in greatest dimension
5 very high	Same as 4, but ≥ 1.5 cm in greatest dimension or definite extraprostatic extension/invasive behavior

T2-weighted and DWI are the major MRI sequences used in assigning a PI-RADS score, with DCE having a smaller role. MR spectroscopy does not play a role in PI-RADS v2.1 scoring. Prostate lesions are characterized using PI-RADS criteria, with DWI the primary imaging sequence for assessment of the peripheral zone and the T2-weighted sequence for the transition zone. (**Figures 8-10** and **Table 5** and **Table 6**). Prostate cancer in the peripheral zone will restrict diffusion, and prostate cancer in the transition zone will appear T2 hypointense with 'erased charcoal' or smudgy, ill-defined margins. There is overlap with stromal T2 hypointense nodules in benign prostatic hypertrophy, but these BPH nodules are typically well defined. However, despite the guidelines, benign conditions can overlap with malignancy, particularly focal prostatitis. **Figure 11**). In addition to false positives, there is also a 10-20% false negative rate for detection of clinically significant cancer[34] at a per lesion level and variation observed in radiologist interpretation of PIRADS scores.[35] Many recent articles have described various MR imaging pitfalls for prostate cancer, thus the PI-RADS v2.1 guidelines is considered a 'fluid' document.

Table 5. PI-RADS v2.1 - Scoring of Peripheral Zone based on DWI, T2W and DCE

DWI	T2W	DCE	PIRADS
1	ANY	ANY	1
2	ANY	ANY	2
3	ANY	-	3
3	ANY	+	4
4	ANY	ANY	4
5	ANY	ANY	5

Table 6. PI-RADS v2.1 - Scoring of Transition Zone based on T2W, DWI and DCE

T2W	DWI	DCE	PIRADS
1	ANY	ANY	1
2	≤ 3	ANY	2
2	≥ 4	ANY	3
3	≤ 4	ANY	3
3	5	ANY	4
4	ANY	ANY	4
5	ANY	ANY	5

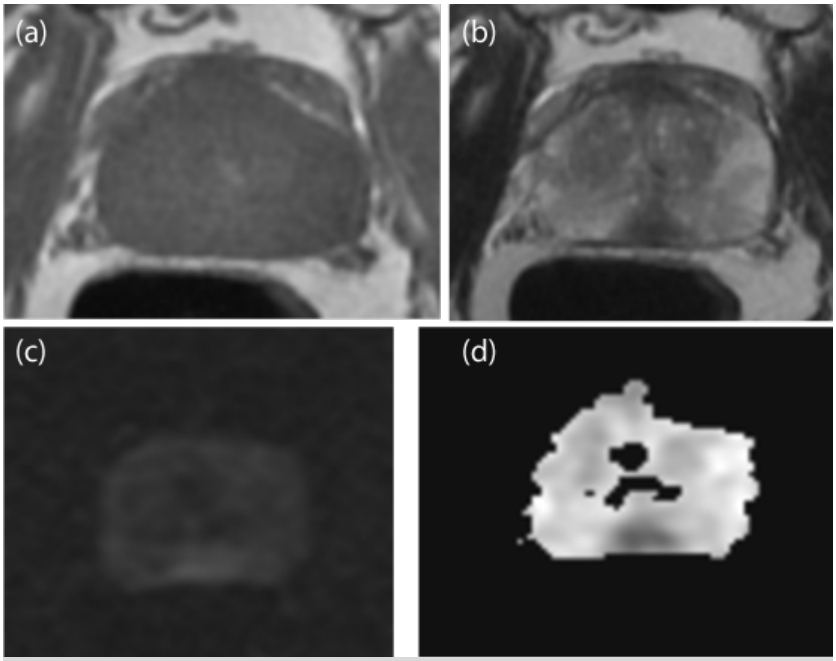

Figure 8: Gleason 8 Prostate Carcinoma on MRI, PSA 10.8. Axial T1 (a) and Axial T2 (b) weighted images demonstrate a hypointense mass in the mid peripheral zone. The mass restricts diffusion as it is bright on high b value (b1200) diffusion weighted imaging (c) and is dark on the ADC map (d)

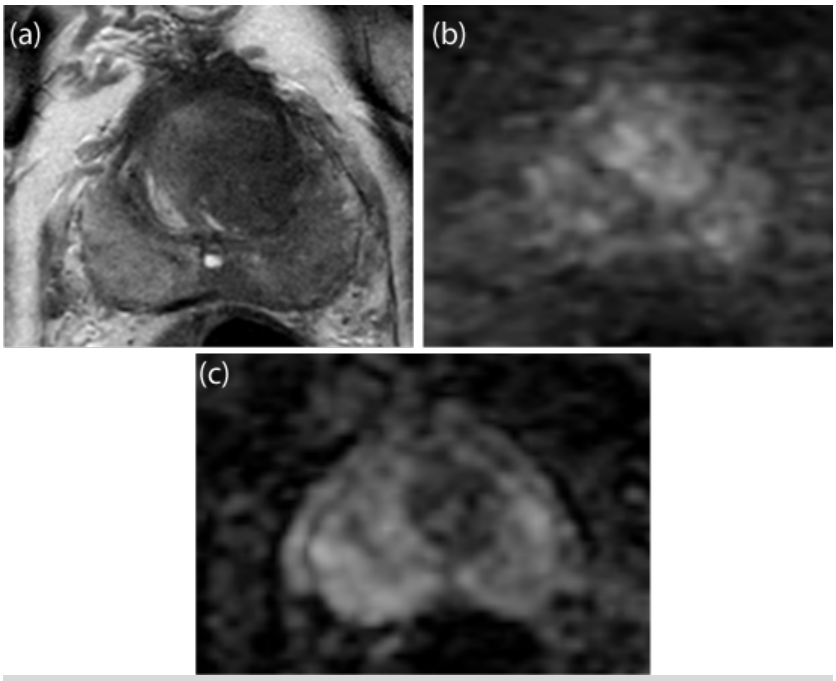

Figure 9: Gleason 7 Prostate Carcinoma in left transition zone on MRI, PSA 25. Axial T2 weighted image (a) demonstrate an hypointense mass (arrows) with ill-defined, “smudgy” lesional margins. The mass restricts diffusion as it is bright on high b value (b1400) diffusion weighted image (arrows) (b) (arrow) and is dark on the ADC map (arrows) (c).

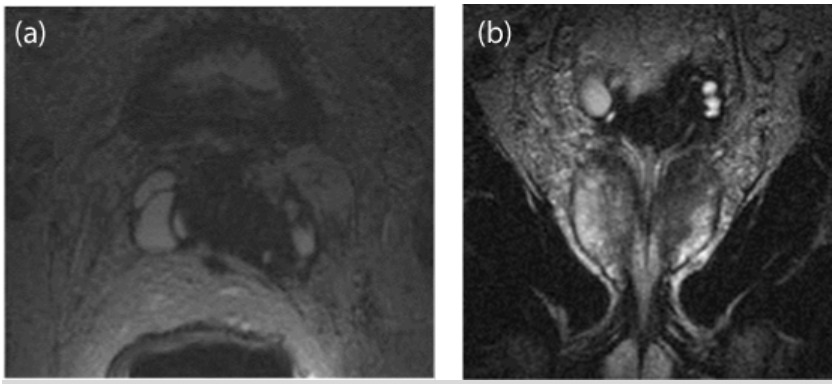

Figure 10: Prostate Carcinoma on MRI. Axial (a) and Coronal (b) T2 weighted images from a different patient with prostate cancer demonstrates extracapsular extension of tumor into the seminal vesicles, left greater than right (arrows).

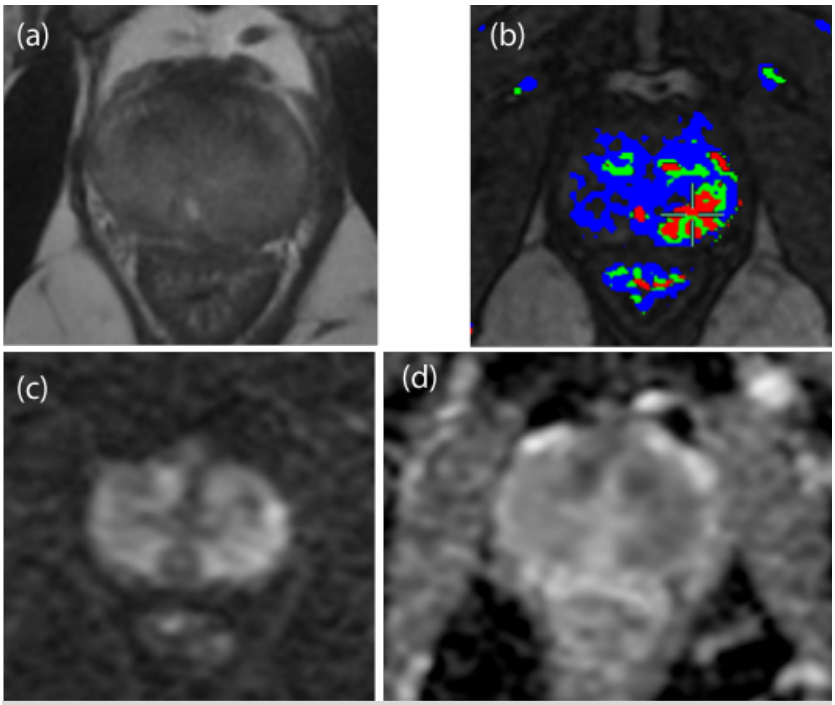

Figure 11. Prostatitis mimicking prostate cancer on MRI. Axial T2 weighted image (a) shows an ill-defined T2 hypointense mass (arrows) in the left peripheral zone that bulges the prostate capsule with irregularity of the prostate capsule raising the possibility for extraprostatic extension. Color map (b) shows focal increased perfusion as an area of 'red' (arrows). B 1200 DWI (c) and ADC map (d) show corresponding area of restricted diffusion. On pathology the findings represented prostatitis.

MRI is indicated in the following situations:

An American College of Radiology Appropriateness Criteria® expert panel indicated the following indications for which mpMRI are indicated for detection and management of prostate cancer:[36]

1. Staging patients at high risk for locally advanced disease and metastases (i.e. PSA ≥ 20 or Gleason 8-10 or clinical stage T2c or higher)
2. Prior negative prostate biopsies in setting of concern for prostate cancer (rising or persistently elevated serum

markers suggesting cancer) for repeat biopsy with MRI fusion (see AUA Core Curriculum: Prostate Cancer)
3. Pre-surgical planning
4. Active surveillance in a patient with known prostate cancer
5. Local recurrence post prostatectomy

The AUA has stated that the use of MRI can be done in men at risk of harboring prostate cancer and who have not undergone a previous biopsy, as well as in men with an increasing prostate specific antigen following an initial negative prostate biopsy.

5. Additional Figures

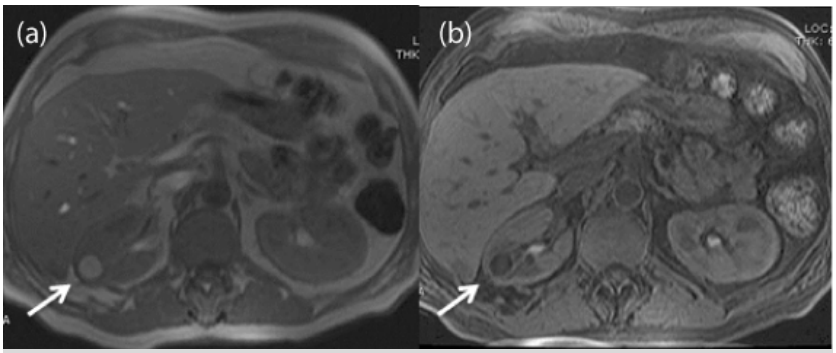

(a) Axial T1-weighted image of a right renal mass with macroscopic fat demonstrated on (b) fat suppression images.

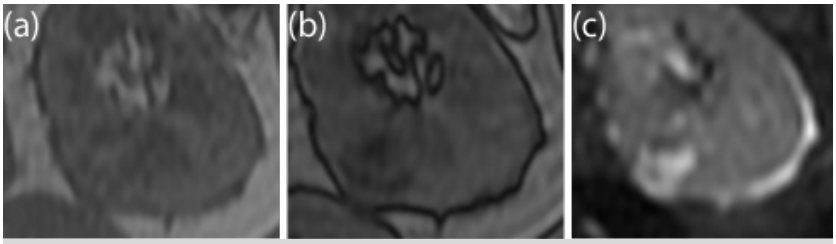

MRI of clear cell renal cell carcinoma shown with (a) in and (b) out of phase imaging as well as restricted diffusion on (c) diffusion weighted MRI.

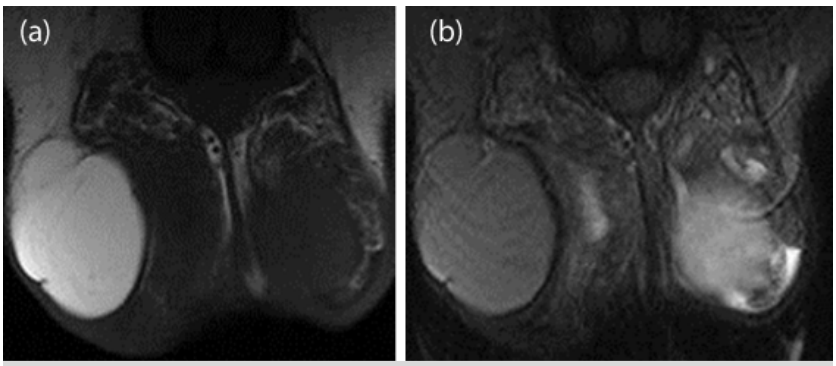

Coronal T1 (a) and Coronal T2 fat suppressed (b) images demonstrate a lobulated right T1 hyperintense mass that homogeneously drops in signal on T2 fat suppressed images in keeping with a scrotal wall lipoma.

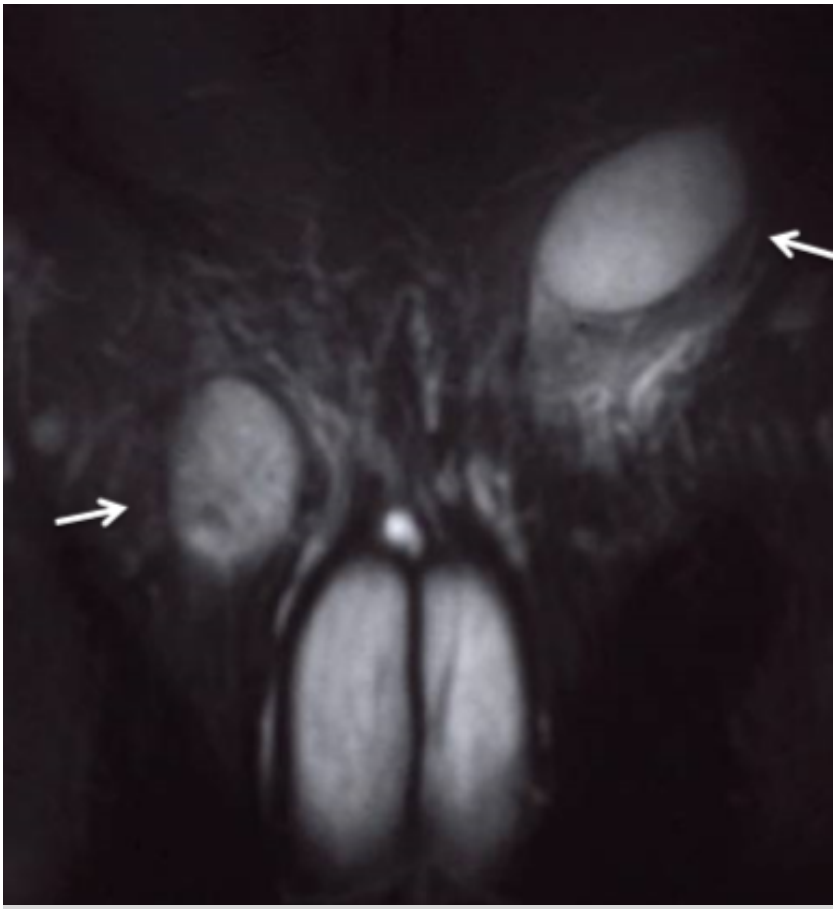

Coronal T2 fat suppressed image of the pelvis demonstrates bilateral undescended testes. The left testis is intra-abdominal and the right testis is in the inguinal canal.

Coronal T1 (a) and Sagittal T1 fat suppressed contrast enhanced images demonstrate a T1 heterogeneous mass containing macroscopic fat in keeping with a left spermatic cord liposarcoma (arrows). Note the normal left testis that is deviated posteriorly on the sagittal image (arrowheads)

Videos

Presentations

MRI Presentation 1

References

1 Adam, A., et al., Grainger and Allison's Diagnostic Radiology: a Textbook of Medical Imaging. 5th ed. 2007, London, UK: Grainger and Allison's Diagnostic Radiology: a Textbook of Medical Imaging.

2 Jung, W., et al., Initial experience with magnetic resonance imaging-safe pacemakers : a review. J Interv Card Electrophysiol, 2011. 32(3): p. 213-9.

3 Bulas, D. and A. Egloff, Benefits and risks of MRI in pregnancy. Semin Perinatol, 2013. 37(5): p. 301-4.

4 Perazella, M.A., Current status of gadolinium toxicity in patients with kidney disease. Clin J Am Soc Nephrol, 2009. 4(2): p. 461-9.

5 Porter KK, King A, Galgano SJ, Sherrer RL, Gordetsky JB, Rais-Bahrami S. Financial implications of biparametric prostate MRI. Prostate Cancer Prostatic Dis. 2019 Jun 25. doi: 10.1038/s41391-019-0158-x. [Epub ahead of print]

6 Choi JW, Moon W-J. Gadolinium Deposition in the Brain: Current Updates. Korean J Radiol. 2019 Jan; 20(1): 134–147.

7 Seo, J.M., et al., Characterization of lipid-poor adrenal adenoma: chemical-shift MRI and washout CT. AJR Am J Roentgenol, 2014. 202(5): p. 1043-50.

8 Schlund, J.F., et al., Adrenocortical carcinoma: MR imaging appearance with current techniques. J Magn Reson Imaging, 1995. 5(2): p. 171-4.

9 Francis, I.R. and M. Korobkin, Pheochromocytoma. Radiol Clin North Am, 1996. 34(6): p. 1101-12.

10 Nikken, J.J. and G.P. Krestin, Magnetic resonance in the diagnosis of renal masses. BJU Int, 2000. 86 Suppl 1: p. 58-69.

11 Scialpi, M., et al., Small renal masses: assessment of lesion characterization and vascularity on dynamic contrast-enhanced MR imaging with fat suppression. AJR Am J Roentgenol, 2000. 175(3): p. 751-7.

12 Sun, M.R., et al., Renal cell carcinoma: dynamic contrast-enhanced MR imaging for differentiation of tumor subtypes--correlation with pathologic findings. Radiology, 2009. 250(3): p. 793-802.

13 Ergen, F.B., et al., MRI for preoperative staging of renal cell carcinoma using the 1997 TNM classification: comparison with surgical and pathologic staging. AJR Am J Roentgenol, 2004. 182(1): p. 217-25.

14 Hindman, N., et al., Angiomyolipoma with minimal fat: can it be differentiated from clear cell renal cell carcinoma by using standard MR techniques? Radiology, 2012. 265(2): p. 468-77.

15 Wehrli NE, Kim MJ, Matza BW, Melamed J, Taneja SS, Rosenkrantz AB. Utility of MRI features in differentiation of central renal cell carcinoma and renal pelvic urothelial carcinoma. AJR Am J Roentgenol. 2013 Dec;201(6):1260-7.

16 Chandarana, H. and V.S. Lee, Renal functional MRI: Are we ready for clinical application? AJR Am J Roentgenol, 2009. 192(6): p. 1550-7.

17 Woo, S., et al., Diagnostic performance of MRI for prediction of muscle-invasiveness of bladder cancer: A systematic review and meta-analysis. Eur J Radiol, 2017. 95: p. 46-55.

18 Panebianco, V., et al., Improving Staging in Bladder Cancer: The Increasing Role of Multiparametric Magnetic Resonance Imaging. Eur Urol Focus, 2016. 2(2): p. 113-121.

19 Rouprêt M, Babjuk M, Böhle A, Burger M, Compérat E, Cowan N, et al. Guidelines on Urothelial Carcinomas of the Upper Urinary Tract. European Assosiacion of Urology 2015. Available: http://uroweb.org/wp-content/uploads/EAU-Guidelines-Upper-Urinary-Tract-Urothelial-Cell-Carcinoma-2015-v1.pdf. Accessed December 15, 2019.

20 Mazen Sudah, Amro Masarwah, Sakari Kainulainen, Marja Pitkänen, Hanna Matikka, Vaiva Dabravolskaite, Sirpa Aaltomaa, Ritva Vanninen. Comprehensive MR Urography Protocol: Equally Good Diagnostic Performance and Enhanced Visibility of the Upper Urinary Tract Compared to Triple-Phase CT Urography. PLoS One. 2016; 11(7): e0158673.

21 Haider, M.A., et al., Combined T2-weighted and diffusion-weighted MRI for localization of prostate cancer. AJR Am J Roentgenol, 2007. 189(2): p. 323-8.

22 ☆ Fulgham PF, Rukstalis DB, Turkbey IB et al.: AUA policy statement on the use of multiparametric magnetic resonance imaging in the diagnosis, staging and management of prostate cancer. J Urol 2017; 198: 832.

23 ☆ Bjurlin MA, Carroll PR, Eggener S, et al. Update of the Standard Operating Procedure on the Use of Multiparametric Magnetic Resonance Imaging for the Diagnosis, Staging and Management of Prostate Cancer. J Urol. 2020;203(4):706-712. doi:10.1097/JU.0000000000000617

24 Kasivisvanathan V, Rannikko AS, Borghi M, Panebianco V, Mynderse LA, Vaarala MH, Briganti A, Budäus L, Hellawell G, Hindley RG, Roobol MJ, Eggener S, Ghei M, Villers A, Bladou F, Villeirs GM, Virdi J, Boxler S, Robert G, Singh PB, Venderink W, Hadaschik BA, Ruffion A, Hu JC, Margolis D, Crouzet S, Klotz L, Taneja SS, Pinto P, Gill I, Allen C, Giganti F, Freeman A, Morris S, Punwani S, Williams NR, Brew-Graves C, Deeks J, Takwoingi Y, Emberton M, Moore CM; PRECISION Study Group Collaborators. MRI-Targeted or Standard Biopsy for Prostate-Cancer Diagnosis. N Engl J Med. 2018 May 10;378(19):1767-1777. doi: 10.1056/NEJMoa1801993. Epub 2018 Mar 18. PMID: 29552975.

25 Bjurlin MA, Carroll PR, Eggener S, et al. Update of the AUA Policy Statement on the Use of Multiparametric Magnetic Resonance Imaging in the Diagnosis, Staging and Management of Prostate Cancer. J Urol. 2019 Oct 23:101097JU0000000000000617. doi: 10.1097/JU.0000000000000617. [Epub ahead of print]

26 Eklund M, Jäderling F, Discacciati A, Bergman M, Annerstedt M, Aly M, Glaessgen A, Carlsson S, Grönberg H, Nordström T; STHLM3 consortium. MRI-Targeted or Standard Biopsy in Prostate Cancer Screening. N Engl J Med. 2021 Jul 9. doi: 10.1056/NEJMoa2100852. Epub ahead of print. PMID: 34237810.

27 Rouvière O, Puech P, Renard-Penna R, Claudon M, Roy C, Mège-Lechevallier F, Decaussin-Petrucci M, Dubreuil-Chambardel M, Magaud L, Remontet L, Ruffion A, Colombel M, Crouzet S, Schott AM, Lemaitre L, Rabilloud M, Grenier N; MRI-FIRST Investigators. Use of prostate systematic and targeted biopsy on the basis of multiparametric MRI in biopsy-naive patients (MRI-FIRST): a prospective, multicentre, paired diagnostic study. Lancet Oncol. 2019 Jan;20(1):100-109. doi: 10.1016/S1470-2045(18)30569-2. Epub 2018 Nov 21. PMID: 30470502.

28 Siddiqui MM, Rais-Bahrami S, Turkbey B, et al. Comparison of MR/Ultrasound Fusion–Guided Biopsy With Ultrasound-Guided Biopsy for the Diagnosis of Prostate Cancer. JAMA. 2015;313(4):390–397. doi:10.1001/jama.2014.17942

29 Ahdoot M, Wilbur AR, Reese SE, Lebastchi AH, Mehralivand S, Gomella PT, Bloom J, Gurram S, Siddiqui M, Pinsky P, Parnes H, Linehan WM, Merino M, Choyke PL, Shih JH, Turkbey B, Wood BJ, Pinto PA. MRI-Targeted, Systematic, and Combined Biopsy for Prostate Cancer Diagnosis. N Engl J Med. 2020 Mar 5;382(10):917-928. doi: 10.1056/NEJMoa1910038. PMID: 32130814; PMCID: PMC7323919.

30 Elkhoury FF, Felker ER, Kwan L, et al. Comparison of Targeted vs Systematic Prostate Biopsy in Men Who Are Biopsy Naive: The Prospective Assessment of Image Registration in the Diagnosis of Prostate Cancer (PAIREDCAP) Study. JAMA Surg. 2019;154(9):811–818. doi:10.1001/jamasurg.2019.1734

31 Christidis, D., et al., Interpreting Prostate Multiparametric Magnetic Resonance Imaging: Urologists' Guide Including Prostate Imaging Reporting and Data System. Urology, 2017.

32 Weinreb, J.C., et al., PI-RADS Prostate Imaging - Reporting and Data System: 2015, Version 2. Eur Urol, 2016. 69(1): p. 16-40.

33 Turkbey B, Rosenkrantz AB, Haider MA, Padhani AR, Villeirs G, Macura KJ, Tempany CM, Choyke PL, Cornud F, Margolis DJ, Thoeny HC, Verma S, Barentsz J, Weinreb JC. Prostate Imaging Reporting and Data System Version 2.1: 2019 Update of Prostate Imaging Reporting and Data System Version 2. Eur Urol. 2019 Sep;76(3):340-351.

34 Samuel Borofsky, Arvin K. George, Sonia Gaur, Marcelino Bernardo, Matthew D. Greer, Francesca V. Mertan, Myles Taffel, Vanesa Moreno, Maria J. Merino, Bradford J. Wood, Peter A. Pinto, Peter L. Choyke, and Baris Turkbey; What Are We Missing? False-Negative Cancers at Multiparametric MR Imaging of the Prostate; Radiology 2018 286:1, 186-195.

35 Geoffrey A. Sonn, Richard E. Fan, Pejman Ghanouni, Nancy N. Wang, James D. Brooks, Andreas M. Loening, Bruce L. Daniel, Katherine J. To'o, Alan E. Thong, John T. Leppert, Prostate Magnetic Resonance Imaging Interpretation Varies Substantially Across Radiologists, European Urology Focus, Volume 5, Issue 4, 2019, Pages 592-599.

36 Expert Panel on Urologic, I., et al., ACR Appropriateness Criteria(R) Prostate Cancer-Pretreatment Detection, Surveillance, and Staging. J Am Coll Radiol, 2017. 14(5S): p. S245-S257.

37 † Perazella MA. Current Status of Gadolinium Toxicity in Patients with Kidney Disease. Clin J Am Soc Nephrol 4: 461–469, 2009.

This is an excellent review of NSF, including patients at risk, mechanisms of pathogenesis and preventive strategies.

38 † Sun MR, Ngo L, Genega EM, Atkins MB, Finn ME, Rofsky NM, Pedrosa I. Renal cell carcinoma: dynamic contrast-enhanced MR imaging for differentiation of tumor subtypes--correlation with pathologic findings. Radiology 250(3):793-802, 2009.

This is a large retrospective study of surgically resected patients who had preop MRI, demonstrating that MRI characteristics accurately distinguished different RCC histologic subtypes.

39 Jung W, Zvereva V, Hajredini B, Jäckle S. Initial experience with magnetic resonance imaging-safe pacemakers: a review. J Interv Card Electrophysiol 32(3):213-9, 2011.

40 Sacco E, Pinto F, Totaro A, D'Addessi A, Racioppi M, Gulino G, Volpe A, Marangi F, D'Agostino D, Bassi P. Imaging of Renal Cell Carcinoma: State of the Art and Recent Advances. Urol Int 86:125–139, 2011.

41 Ergen FB, Hussain HK, Caoili EM, Korobkin M, Carlos RC, Weadock WJ, Johnson TD, Shah R, Hayasaka S, Francis IR. MRI for preoperative staging of renal cell carcinoma using the 1997 TNM classification: comparison with surgical and pathologic staging. AJR Am J Roentgenol 182(1):217-25, 2004.

42 Brown RFJ, Tuite DJ. Imaging of the renal transplant: comparison of MRI with duplex sonography. Abdom Imaging 31:461–482, 2006.

43 Chandarana H, Lee VS. Renal functional MRI: Are we ready for clinical application? AJR Am J Roentgenol 192(6):1550-7, 2009.

44 Adam, Andy. Grainger & Allison's Diagnostic Radiology A Textbook of Medical Imaging. 5th ed. Philadelphia: Churchill Livingstone, 2008.

45 Scialpi M, Di Maggio A, et al. Small Renal Masses AJR AM J Roentgenol 2000 175:3, 751-757

46 Haider Ma, van der Kwast TH, et al. Combined T2-Weighted and Diffusion-Weighted MRI for Localization of Prostate Cancer. AJR AM J Roentgenol 2007 189:2.323-328.

47 Koh D and Collins DJ. Diffusion-Weighted MRI in the Body: Applications and Challenges in Oncology. AJR AM J Roentgenol 2007;188: 1622-1635.

48 Weinreb JC, Barentsz JO, Choyke PL, Cornud F, Haider MA, Macura KJ, Margolis D, Schnall MD, Shtern F, Tempany CM, Thoeny HC, Verma S. Weinreb JC. PI-RADS Prostate Imaging-Reporting and Data System:2015,Version 2. Eur Urol 2016;69(1):16-40.

49 Hindman N, Long N, Genega EM, et al. Angiomyolipoma with Minimal Fat: Can It Be Differentiated from Clear Cell Renal Cell Carcinoma by Using Standard MR Techniques? Radiology. 2012;265:468-77.

50 American College of Radiology ACR Appropriateness Criteria

51 Characterization of Lipid-Poor Adrenal Adenoma: Chemical-Shift MRI and Washout CT. Seo JM, Park BK, Park SY, and Kim CK. American Journal of Roentgenology 2014 202:5, 1043-1050.